Journal of Ceramic Processing Research. Vol. 14, No. 3, pp. 385~390 (2013)

J O U R N A L O F
Ceramic Processing Research

Synthesis and structural properties of DC sputtered AlN thin films on different substrates

S. Shanmugan[a,*], D. Mutharasu[a], P. Anithambigai[a], N. Teeba[a] and I. Abdul Razak[b]

[a]*Nano Optoelectronics Research Laboratory, School of Physics, Universiti Sains Malaysia (USM),11800, Minden, Pulau Penang, Malaysia*

[b]*X-ray crystallography Laboratory, School of Physics, Universiti Sains Malaysia (USM), 11800, Minden, Pulau Penang, Malaysia*

Aluminum Nitride thin films were prepared over different substrates using DC sputtering at room temperature. The prepared films were mostly *c*-axis oriented on Al substrates. Poor crystalline were recorded for both glass and Si substrates. Cu substrates supported the growth of cubic (2 0 0) AlN. Annealing process showed noticeable effect on *c*-axis AlN prepared over Al substrates. The observed crystallite sizes were between 9 nm and 79 nm. The applied stress during the growth were tensile nature and showed high value for (1 1 0) phase on Al substrates. The structural parameters such as dislocation density, micro strain etc., were dependent not only the orientation of AlN crystals but also the substrates used. Annealing process showed noticeable reduction on residual stress and micro strain and improvement on crystallite growth as well as the dislocation density.

Key words: AlN, Thin films, Structural properties, Sputtering.

Introduction

The solar collector tubes in solar thermal electricity plants use Mo-Al_2O_3 cermet as the solar absorber, because of the excellent thermal stability of the material at the high operating temperatures of 450-500 °C in vacuum. A solar absorptance of 0.96 and emittance of 0.16 at 350 °C have been achieved. However, the deposition rate is lower [1] and the cost of deposition equipment using planar magnetron technology is much higher, compared to reactively sputtered stainless steel-carbon (SS-C) [2, 3] and Al-N cermet solar coatings [4-7]. The Mo-Al_2O_3 cermet solar coatings are therefore more expensive compared with dc reactively sputtered SS-C and Al-N cermet solar coatings which are also produced using a commercial-scale cylindrical dc sputtering coater. Aluminum nitride (AlN) has generated much interest than SS-C due to its unique properties of wide band gap of 6.2 eV, high thermal conductivity (320 $Wm^{-1} K^{-1}$) [8], low thermal expansion coefficient, high chemical and thermal stabilities, high breakdown dielectric strength, and high surface acoustic wave velocity [9-11].

A variety of deposition methods for the AlN films have been reported, e.g. reactive sputtering [12], reactive evaporation [13] metal-organic chemical vapor deposition (MOCVD) [14], laser-molecular beam epitaxy [15], pulsed laser deposition (PLD) [16], arc discharge method [17], and chloride-assisted chemical vapor deposition [18]. Among this method, reactive sputtering is relatively good and low cost method for the preparation of AlN thin film.

In a reactive-sputtering process, molecules of a reactive gas combine with the sputtered atoms from a metal target to form a compound thin film on a substrate. Due to the affinity of AlN thin film for oxygen [19], AlN films may contain a surface oxide layer, which greatly influences the physical properties, and can modify the electronic structure and promote shifts in luminescence peaks [20, 21]. The luminescence properties of AlN are determined mainly by the presence of oxygen impurities in the host lattice [22]. The texture of these films, however, is strongly dependent on the texture and smoothness of the substrate material, which necessitates the study and optimization of AlN growth on conducting thin films suitable for bottom electrodes [23]. This work focuses on the deposition of thin AlN films on different substrates (Cu, Al, glass, Si). The selection of substrates is based on the material used for solar thermal as well as electrical applications. The structural properties such as crystallite size, dislocation density, internal stress, etc., of all prepared samples are also reported here.

Experimental Methods

AlN thin films were deposited on different substrates (Glass, Al, Cu and Si) using Al (99.99% purity) target (3 inch in diameter and 4 mm in thickness) by DC sputtering (Edwards make, Model-Auto 500). The chamber was initially evacuated to high vacuum 8.2×10^{-6} mbar by using a turbo molecular pump backed by a rotary pump and fixed as base pressure for coating. High pure Ar (99.999%) and N_2 (99.999%) were used for AlN

*Corresponding author:
Tel : +60-04-6533672
Fax: +60-04-6579150
E-mail: subashanmugan@gmail.com

coatings. Ar and N_2 gas mixture ratio was fixed as 60 : 40 (13 sccm : 7 sccm with total of 20 sccm). The substrates were cleaned by rinsing in ultrasonic bath of acetone and isopropyl alcohol. All AlN thin films were coated at room temperature and the thickness of the film was 325 nm measured by digital thickness monitor. The deposition rate and sputtering power were kept constant at 0.42 Å / sec and 200 W, respectively. In order to remove the surface oxidation of the target, pre-sputtering was carried out for 5 min before starting deposition at Ar pressure of 3.2×10^{-3}. To get the uniform thickness, rotary drive system was used and 25 RPM was fixed for all AlN film coatings. All AlN thin films were coated at chamber pressure of 8.2×10^{-3}. Substrate to target distance of 7 cm was kept constant for all depositions. Annealing process were carried out for all samples at 400 ºC for 3 hrs duration in N_2 gas atmosphere.

The crystalline nature of the as-grown and annealed AlN thin films was investigated by using a high resolution X-ray diffraction (HRXRD, X'pert-PRO, Philips, Netherlands). A CuKα (λ = 1.54056 Å) source was used, with a scanning range between 2θ = 33 º and 70 º. This range has been selected because of most of AlN peaks were observed between this ranges.

Results and Discussion

Structural properties

XRD spectra of all as grown AlN samples are recorded as shown in fig. 1. The observed results are compared with standard JCPDS file. It shows that the glass, Si and Al substrates exhibit only the hexagonal phase of AlN. The observed peaks are assigned to be a wurtzite hexagonal phase (group 186, file 00-025-1133) with lattice parameter a = 3.11 Å, c = 4.97 Å [24]

From fig. 1, all substrates show very low intensity of (1 0 0) oriented peak when compared to (1 0 3) oriented peak before and after annealing which exhibit the synthesized film is *c*-axis normal to the substrate [25].

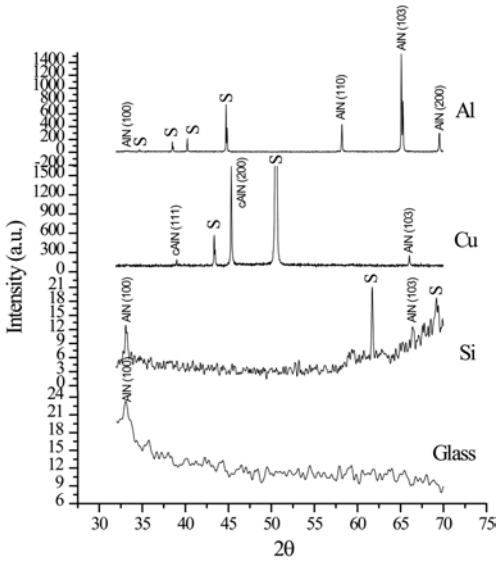

Fig. 1. XRD spectra of as grown AlN thin film on different substrates (S denotes substrates peaks).

From the observed mixed phases, an AlN thin film grown on Cu, Al, Si, and glass substrates are not epitaxially well along their axis. The XRD spectra also suggest that the crystal orientation as well as the crystallinity of the AlN films depends on the substrates used [26].

From Fig. 1, it also reveals that the mixed phases (cubic and hexagonal) are observed in Cu substrates. Very low intensity (1 0 0) peaks are observed for AlN thin film prepared over glass, Si and Al substrates. But only (0 0 2) oriented peak has been reported for AlN on (1 0 0) Si by rf sputtering in different work [27]. It seems that there is not much improvement on the growth of (1 0 0) oriented AlN phase even it is coated on different substrates. But (2 0 0) phase of AlN is observed only on Al substrates. In addition to this, Al substrate enhances the crystallinity of (1 0 3) oriented AlN when compared to other substrates. Moreover, cubic phase are dominated in Cu substrates especially

Table 1. Structural parameters of as grown AlN thin film over different substrates

Substrate	2 theta	Std. 2 theta	*d*	Std. *d*	*hkl*	FWHM (θ)	Crystallite size (nm)	Residual stress × 10^{-3}	JCPDS File No.
Glass	32.93	32.97	2.716	2.714	h100	0.037	40.81	-0.033	700354
Si	33.08	33.10	2.707	2.705	h100	0.084	17.98	-0.033	893446
	66.39	66.59	1.416	1.403	h103	0.040	43.26	-0.414	882360
Cu	39.05	39.42	2.305	2.284	c111	0.074	20.76	-0.411	650841
	45.40	45.84	1.996	1.978	c200	0.094	16.7	-0.406	650841
	66.08	66.08	1.414	1.413	h103	0.057	30.31	-0.032	650831
Al	33.26	33.22	2.692	2.695	h100	0.029	52.1	0.050	251133
	58.23	58.87	1.583	1.568	h110	0.092	18.02	-0.427	700354
	65.16	65.71	1.431	1.420	h103	0.176	9.76	-0.346	700779
	69.58	69.45	1.350	1.352	h200	0.107	16.48	0.066	893446

(2 0 0) orientation. It reveals that the possibility of cubic phase growth is more on Cu substrates when AlN growth at room temperature than other substrates. From this observation, cubic Al substrates enhance the growth of (1 0 3) oriented hexagonal AlN than cubic Cu and hexagonal Si substrates. However, cubic copper substrates enhance the growth of cubic (2 0 0) oriented AlN than hexagonal (1 0 3) phase of AlN. It is attributed to the lesser mismatch between the cubic Cu substrates and cubic AlN and hence suppress of hexagonal AlN growth is observed on Cu substrates [28].

The observed FWHM is an indication of crystallinity of the prepared samples. From the Table 1, it clearly indicates that the crystallinity depends only on the orientation of the crystal on selective substrates. Table 1 shows that the prepared AlN thin film with (1 0 3) and (2 0 0) orientation over Al substrates are poor crystallinity when prepare at room temperature. The crystal orientation of the substrates also influences the oriented growth of AlN thin film. The substrates used for AlN growth are cubic (Cu and Al) and hexagonal (Si) phase. From the Table 1, Cu substrate helps to grow cubic AlN phase than hexagonal AlN. Unfortunately, hexagonal Si does not support the hexagonal AlN. The same behavior was already reported for different metal electrodes by M. Akiyama et al. [26]

In order to understand in detail, the peak position analysis is also carried out. The observed and standard peak positions for comparison are given in Table 1. It clearly indicates that all observed peak positions except (1 0 0) and (2 0 0) phases on Al shift towards left from the standard positions from JCPDS file data. In addition, the influence of heat on the growth of AlN thin film was also analyzed by recording XRD spectra of AlN thin film samples annealed at 400 °C for 3 hrs in presence of N_2 gas (see fig. 2). Form Fig. 2, it shows

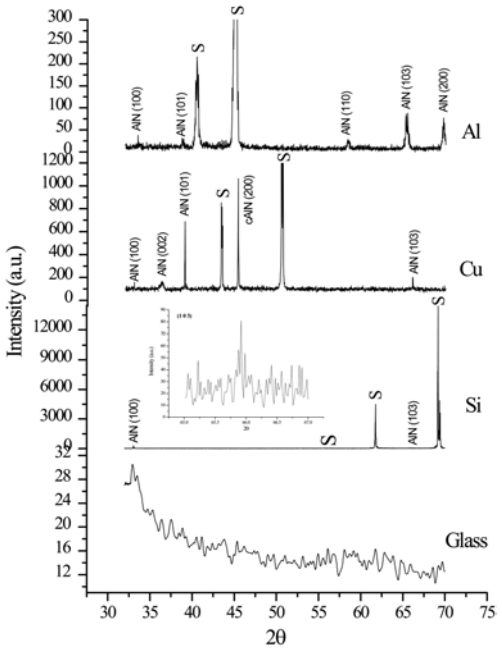

Fig. 2. XRD spectra of AlN thin film on different substrates annealed at 400 °C for 3 hrs duration. (S denotes substrates peaks).

that the (1 0 0) phases of AlN are exist in all substrates and the intensity of (1 0 0) phase is very low for both glass and Si than other substrates. No other phases related to AlN are observed for glass substrates even after annealing. On considering Si substrates, annealing process helps to increase the intensity of (1 0 0) phase noticeably. The inset fig shows the XRD spectrum of (1 0 3) phase of AlN on Si substrate. Fig. 2 also reveals that the annealing process shows no influence on cubic (2 0 0) phase and a small decrease on (1 0 3) phase. But it is also depicts that few new *c*-axis oriented hexagonal (002) phase and (1 0 1) phase are observed. A phase transition from cubic (1 1 1) phase to hexagonal

Table 2. Structural parameters of AlN thin film over different substrates annealed at 400 °C for 3 hrs duration.

Substrate	2 theta	Std. 2 theta	*d*	Std. *d*	*hkl*	FWHM (θ)	Crystallite size (nm)	Residual stress × 10^{-3}	JCPDS File No.
Glass	32.92	32.97	2.718	2.714	h100	0.032	47.19	-0.066	700354
Si	33.06	33.10	2.707	2.705	h100	0.036	41.96	-0.033	893446
	65.87	65.89	1.418	1.416	h103	0.022	78.44	-0.063	893446
Cu	33.08	33.10	2.706	2.705	h100	0.027	55.95	-0.017	893446
	36.32	36.30	2.472	2.473	h002	0.025	60.96	0.018	871054
	45.40	45.84	1.996	1.978	c200	0.046	34.13	-0.406	650841
	66.04	66.06	1.414	1.413	h103	0.076	22.73	-0.032	760702
Al	33.47	33.53	2.675	2.671	h100	0.020	75.61	-0.067	882360
	38.74	38.29	2.323	2.349	h101	0.061	25.16	0.494	871054
	58.50	58.87	1.576	1.568	h110	0.021	79.04	-0.228	700354
	65.50	65.71	1.424	1.420	h103	0.036	47.83	-0.126	700779
	69.75	69.73	1.347	1.348	h200	0.024	73.55	0.033	251133

phase could be observed by annealing process.

The annealing process has immense effect on the growth of AlN on Al substrates as reduce the crystalline quality by observing low intensity of AlN peaks from the as grown samples. In addition, a (1 0 1) phase is observed for annealed AlN samples coated over Al. it reveals that the annealing of DC sputtered AlN thin film in presence of N_2 gas supports the growth of (1 0 1) phase when prepared on metal substrates. Overall, the crystalline quality of hexagonal AlN thin films prepared over Al substrate are comparatively good in as grown condition. The annealing process helps to increase the crystalline quality for AlN thin film coated over Si and Cu substrates. The same behavior of improved crystalline quality on Si has already been reported by H. Takikawa et al. [25]

In peak position analysis, all hexagonal peaks related to AlN except (0 0 2) phase on Cu and (1 0 1) & (2 0 0) phase on Al exist at lower 2θ than the standard one. The shift in peak position is also an indication of structural defects as the applied stress during the growth. From Table 1 & 2, it is observed that most of the films are under tensile stress [29]. This could be verified by analyzing the residual stress in the consecutive section. The observed values are compared with standard JCPDS file as given in Table 2.

In order to investigate the possibility of preferred orientation, the Harris analysis [30] was performed using the following relationship for the texture coefficient (TC).

$$P_i\ (TC) = N\ (I_i/I_0) / \Sigma^N_{i=1}(I_i/I_0) \quad (1)$$

where P_i is the texture coefficient of the plane I, I_i is the measured intensity, I_0 is the intensity of the JCPDS powder diffraction pattern of the corresponding peak and N is the number of reflections considered for the analysis. P_i is unity for each reflection in the case of a randomly oriented sample and values of P_i greater than unity indicate preferred orientation of the crystallites in that particular direction. The calculated TC values for all as grown samples are given in Table 1. It shows that the preferred oriented growth of (1 0 3) and (2 0 0) AlN phases are observed on Al substrates. In addition, the (1 0 3) phase also shows the preferred growth on Al substrates. However, (1 0 0) phase is randomly oriented on Si and Al substrates. From Table 2, the calculated TC values of the annealed samples evidence the growth of AlN on their preferred (2 0 0) orientation on Al substrate. However, noticeable reduction on TC value could also be observed for other substrates even after annealing process.

The crystallite size (D) was calculated using the Debye Scherer formula [31] from the Full-Width at Half-Maximum (w) measurements:

$$D = 0.94\lambda / w\ cos\theta \quad (2)$$

where λ is the wavelength of incident X-ray. The calculated crystallite size for as grown AlN thin films is given in Table 1. The orientations such as (1 0 0), (1 0 3), and (2 0 0) of AlN peaks are considered in this discussion. The table reveals that the calculated crystallite size is less than 100 nm. Low (9.76 nm) value in crystallite size is observed for the (1 0 3) orientation of AlN which is coated over Al substrates and high value (52.1 nm) is observed for (1 0 0) oriented AlN which is coated over Al substrates. By calculating the average crystallite size of hexagonal phase, AlN thin film coated over Al substrates has low crystallite size of about 24 nm. High value of about 41 nm is observed with glass substrates.

In order to evaluate the influence of heat, the crystallite size of annealed AlN thin films is calculated and given in Table 2. It shows that the low value (22.73 nm) as well as high value (79 nm) are observed for (1 0 3) orientation of AlN coated on Cu and (1 1 0) orientation on Al substrates respectively. In addition, particularly for (1 0 0) orientation, variation in crystallite size is minimum for the AlN thin films coated over Glass, Si and Cu substrates. The average crystallite size of AlN over different substrates is as follows: Glass - 47.2 nm, Si - 60 nm, Cu - 46 nm, and Al - 60 nm. Overall, an increase in crystallite size is observed by annealing process. Generally, raising the temperature gives the deposited atoms an extra mobility, allowing them to reach the lowest thermodynamically favored lattice positions hence, the crystal size becomes larger and the crystallinity of the film improves [32]. However, a noticeable decrease in crystallite size could be observed for (1 0 3) on Cu after annealing process. This may be due the influence of substrate on the particular orientation of AlN.

The internal stress (σ) in the processed samples is calculated using the relation

$$\sigma = -\ E\ (d_a - d_o) / (2d_oY) \quad (3)$$

where d_o and d_a are the d spacing of bulk and thin film forms respectively. E and Y are the Young's modulus and Poisson's ratio of AlN respectively. The Young's modulus and Poisson's ratio of AlN are $E = 308$ GPa [33] and $Y = 0.29$ [34] respectively. The calculated internal or residual stress is also given in Table 1 and 2. Table 1 shows the results observed for as grown AlN thin film over different substrates. From Equation - 3, the nature of stress applied during the growth of crystal could be identified by the sign of the observed value. If the observed value is in positive, it represents the compressive stress and if it is negative, the tensile stress is applied during the growth process. Hence the applied stress during the growth for all samples except (1 0 0) and (2 0 0) phase observed for Al substrates are tensile nature. The applied stress value for (1 0 0) phase is similar for glass and Si substrates. However, the applied stress was compressive for (1 0 0) and (2 0 0) phases of AlN thin films prepared over Al substrates. For (1 0 3) phase, a noticeable drastic reduction on tensile

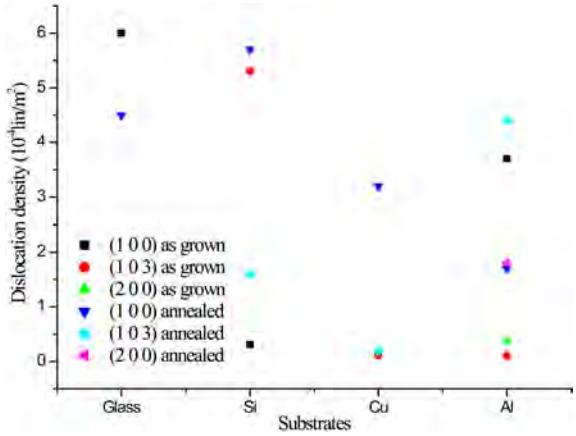

Fig. 3. Change in dislocation density of as grown and annealed AlN thin film samples on different substrates with respect to orientations.

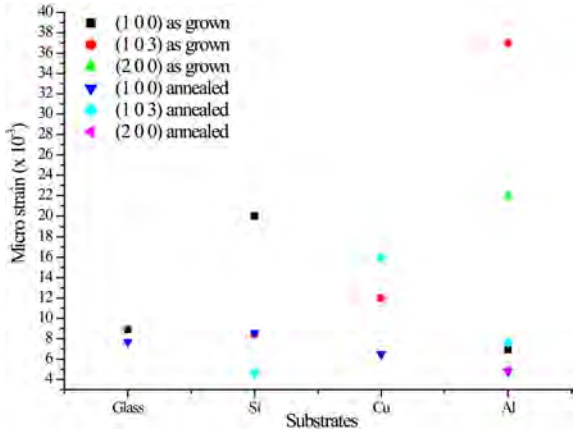

Fig. 4. Change in micro strain of as grown and annealed AlN thin film samples on different substrates with respect to orientations.

stress could be observed for AlN coated over Cu substrates than Si substrates.

As discussed before, the effect of heat on the internal stress developed as a result of annealing are discussed here. The calculated values of internal stress for annealed samples are given in Table 2. The applied stress for all samples is mostly observed as tensile except (0 0 2) phase for Cu and (1 0 1) and (2 0 0) phases for Al substrates.

When compare with as grown samples, the annealing process does not show any changes on internal stress for (1 0 0) and (1 0 3) phases for AlN thin film coated over Si and Cu substrates respectively. An increase in internal stress could also be observed for (1 0 0) phase of AlN thin film from Glass substrate. In addition, a stress conversion from compressive to tensile is observed for (1 0 0) AlN on Al substrate. For (1 0 3) phase, a noticeable reduction in internal stress could be observed for both Si and Al substrates. In addition, 50% of the stress is reduced as a result of annealing when the (2 0 0) AlN on Al substrates.

To strengthen the above discussion, the dislocation density (δ) defined as the length of dislocation lines per unit volume of the crystal is evaluated from the formula [35].

$$\delta = 1/D^2 \tag{4}$$

The calculated δ values for as grown AlN thin film over different substrates are plotted in Fig. 3. Overall, the figure shows noticeable variation on dislocation density depending on the substrates for AlN thin film synthesis. As a result of annealing, it exhibit that a huge increase in dislocation density is observed for (1 0 0) and (1 0 3) phases of AlN on Si and Al substrates respectively. It also reveals that the dislocation density value for (1 0 0) on Si, (1 0 3) on Cu and Al, and (2 0 0) on Al is low when compared with annealed AlN thin film. In addition, a small change in δ value is observed for (1 0 3) phase of AlN synthesized over Cu substrates. It is also observed that (1 0 3) phase on Cu and Al substrates show low dislocation density value than other substrates. It seems to be the behavior of low misfit between hexagonal AlN and cubic substrates. The annealing process contributes to decrease in d value for (1 0 0) and (1 0 3) phases on glass & Al and Si substrate respectively.

It is known that the crystallite size is indirectly proportional to micro strain denoted as follows:

$$D = 0.94\lambda / 4\varepsilon \tag{5}$$

and the strain (ε) was calculated from the following formula

$$\varepsilon = w \cos\theta / 4 \tag{6}$$

The calculated strain for all samples is plotted in Fig. 4. It shows that the (1 0 3) phase of AlN on Al substrates exhibit higher value compared to other samples. It may be due to the lattice mismatch between hexagonal (1 0 3) phase of AlN and cubic (1 1 1) phase of Al substrates. A drastic reduction on strain could also be observed for the same (1 0 3) phase when the sample undergoes annealing process. Figure 4 also reveals the decreasing manner of strain for (1 0 0) phase coated on glass, Si, Al, and (2 0 0) phase coated on Al due to annealing process. A noticeable reduction on micro strain is observed for (1 0 0) on Si as for (1 0 3) phase on Al. In addition, the annealing process helps to increase the strain value for (1 0 3) phase of AlN coated on Cu substrates. Overall, the annealing process contributes on reducing the micro strain considerably. Lower value in micro strain as a result of annealing is observed for both Si and Al substrates.

Conclusions

DC sputtered AlN thin films were synthesized on different substrates. AlN thin film synthesized over glass and Si substrates were in poor crystalline nature. The polycrystalline AlN with different orientations were observed on Si, glass and Al substrates. Mixed phases

of cubic and hexagonal orientation were observed for AlN prepared on Cu substrates. Highly textured and preferred oriented AlN thin films were grown on Al and Cu substrates. Cu substrates supports the growth of cubic (2 0 0) phase of AlN. Annealing process showed an immense effect of AlN phases grown over Al substrates. The observed crystallite size of AlN thin films were < 100 nm before and after annealing. The structural parameters were depending upon the orientations of the AlN thin films with respect to substrates. The calculated dislocation density was high for (1 0 0) on glass and low for (1 0 3) on Al substrates. Cubic (2 0 0) of AlN on Cu showed high dislocation density for annealing. The applied stress for as grown was tensile nature and also changed with respect to substrates.

Acknowledgment

The authors would like to thank the Nano-Optoelectronics Research Laboratory in School of Physics where all AlN thin film samples were synthesized by using DC sputtering system and the XRD lab for providing the crystallographic analysis facilities.

References

1. J.A. Thornton, in "sputter deposition processes" (Handbook of Deposition Technologies for Films and Coatings, ed. R. F. Bunshah. Noyes Publications, U.S.A, 1994) p. 249.
2. Q,-c. Zhang, Sol. Ener. Mater. Sol. Cells 52 [1-3] (1988) 95-106.
3. G,-l. Harding, B. Window, D,-r. McKenzie, A,-r. Collins, C,-m. Horwitz, J. Vac. Sci. Technol. 16 (1979) 2105-2108.
4. Q,-c. Zhang, J. Phys. D: Appl. Phys. 31 (1988) 355-362.
5. Z. Yin, G,-l. Harding, Thin Solid Films 120 [2] (1984) 81-108.
6. B. Window, G,-l. Harding, Solar Energy 32 [5] (1984) 609-623.
7. S. Hou, in SPIE 1727 Proceedings of Optical Materials Technology for Energy Efficiency and Solar Energy Conversion X, May 1992, edited by A.H.-L. Goff and C. M. Lampert (Toulouse-Labege, France 1992) p. 240.
8. A. Jacquot, B. Lenoir, A. Dauscher, P. Verardi, F. Craciun, M. M. Stölzer, M. Gartner, and M. Dinescu, Appl. Surf. Sci. 186 [1-4] (2002) 507-512.
9. H. Yamashita, K. Fukui, S. Misawa, S. Yoshida, J. Appl. Phys. 50 [2] (1979) 896-898.
10. G,-a. Slack, R,-a. Tanzilli, R,-o. Pohl, J,-w. Vandersande, J. Phys. Chem. Sol. 48 [7] (1987) 641-647.
11. J. Ohta, H. Fujioka, S. Ito, M. Oshima, Appl. Phys. Lett. 81 [13] (2002) 2373-2375.
12. G,-f. Iriarte, F. Engelmark, and I,-v. Katardjiev, J. Mater. Res., 17 [6] (2002) 1469-1475.
13. R. Bensalem, A. Abid, B,-j. Selly, Thin Solid Films 143 (1986) 141-13.
14. H. Amano, N. Sawasaki, I. Akasaki I, Toyoda, Appl. Phys. Lett. 48 [5] (1986) 353-355.
15. Schenk HPD, U. Kaiser, G,-d. Kipshidze, A. Fissel, H. Hobert, J. Schulze, and W. Richter, Mater. Sci. Eng. B 59 [1] (1999) 84-87.
16. C. Ristoscu, C. Ducu, G. Socol, F. Craciunoiu, I,-n. Mihailescu, Appl. Surf. Sci. 248 [1-4] (2005) 411-415.
17. L,-h. Shen, X,-f. Li, J. Zhang, Y,-m. Ma, F. Wang, G. Peng, Q,-l. Cui, G,-t. Zou, Appl. Phys. A 84 [1-2] (2006) 73-75.
18. X. Song, Z. Guo, J. Zheng, X. Li, Y. Pu, Nanotechnology 19 (2008) 115609-115615.
19. V,-a. Lavrenko, J. Desmaison, A,-d. Panasyuk, and M. Deismaison-Brut, J. Eru. Ceram. Soc. 23 (2003) 357-369.
20. G,-a. Slack, L,-j. Schowalter, D. Moreli, and J,-a. Freiats Jr., J Crys. Growth. 246 (2002) 287-298.
21. F. Ansart, H. Ganda, R. Saporte, and J,-p. Traverse, Thin Solid Films 260 [1] (1995) 38-46.
22. L. Trinkler, B. Berzina, A. Auzina, M. Benabdesselan, and P. Lacconi, Nucl. Instrum. A, 580 [1] (2007) 354-357.
23. H.-P. Lobl, in Proceedings of the IEEE Ultrasonic Symposium, October 1999 (Caesars Tahoe, NV 1999) p. 1031.
24. Powder diffraction file, JCPDS International Centre for Diffraction Data, ICDD, Newtown Square, PA, 2003.
25. H. Takikawaa, K. Kimuraa, R. Miyanoa, T. Sakakibaraa, A. Bendavidb, P,-j. Martinb, A. Matsumuroc, K. Tsutsumid, Thin Solid Films 386 [2] (2001) 276-280.
26. M. Akiyamaa, K. Nagaob, N. Uenoa, H. Tateyamaa, T. Yamadab, Vacuum 74 [3-4] (2004) 699-703.
27. J,-x. Zhang, H. Cheng, Y,-z. Chen, A. Uddin, S. Yuan, S,-j. Geng, S. Zhang, Surf. Coat. Technol. 198 (2005) 68-73.
28. M. Kakuda, K. Makino, T. Ishida, S. Kuboya, and K. Onabe, Phys. Stat. Sol. C 9 [3-4] (2012) 558-561.
29. H,-c. Barshilia, B. Deepthi, K,-s. Rajam, Thin Solid Films 516 [12] (2008) 4168-4174.
30. C,-s. Barret, T,-b. Massalski, Structure of Metals, Oxford, Pergamon (1980) p. 204.
31. G. Gordillo, J,-m. Florez, L,-c. Hernandez, Sol. Energy Mater. Sol. Cells 37 [3-4] (1995) 273-281.
32. M,-g. Mendez, S,-m. Rodriguez, S. Shaji, B. Krishnan, P,-b. Perez, Surf. Rev. Lett. 18 [1-2] (2011) 23-31.
33. D. Gerlich, S,-l. Dole, G,-a. Slack, J. Phys. Chem. Solids 47 [5] (1986) 437-441.
34. Thokala, R, Chaudhuri J. Thin Solid Films 266 [2] (1995) 189-191.
35. G,-b. Williamson, R,-e. Smallman, III. Philos. Mag. 1 (1956) 34-45.